Hydrology: Current Research

Ezzeldin et al., Hydrol Current Res 2018, 9:1
DOI: 10.4172/2157-7587.1000297

Research Article Open Access

Comparison between Structured and Unstructured MODFLOW for Simulating Groundwater Flow in Three-Dimensional Multilayer Quaternary Aquifer of East Nile Delta, Egypt

Mohsen M Ezzeldin*, **Kassem S El-Alfy, Hossam A Abdel-Gawad and Mahmoud E Abd-Elmaboud**

Department of Irrigation and Hydraulics, Mansoura University, Egypt

***Corresponding author:** Mohsen M Ezzeldin, Department of Irrigation and Hydraulics, Mansoura University, Egypt, Tel: 020502085262; E-mail: Mahmoud_elsayed717@yahoo.com

Received date: March 02, 2018; **Accepted date:** March 15, 2018; **Published date:** March 26, 2018

Abstract

This study presents the differences and similarities between the MODFLOW-USG (Unstructured Grid version of MODFLOW) and traditional structured versions of MODFLOW 2005 in simulating a three-dimensional multilayer groundwater flow model in Quaternary aquifer east Nile delta in Egypt. A 390-borehole dataset was used to build a three-dimension stratigraphic model of the Quaternary aquifer. GIS-based conceptual model is mapping to represent the different boundary conditions such as lakes, river, drains, aquifer recharge, and discharge. The conceptual model is exported to the stratigraphic model; therefore, boundary conditions data are automatically arranged in arrays identical with the grid cells. MODFLOW 2005 and MODFLOW USG are combined with the computer-based program PEST to calibrate groundwater head distribution through the aquifer system. Groundwater levels measured in 1991 are used for the steady-state calibration and are employed then as initial conditions for the transient calibration between 1991 and 2004. The heads measured in 2015 are used for more model verification. The results show that MODFLOW-USG provides flexibility in grid design, including the capability to use nonrectangular cell shapes. Also, it can be used with simple grids and nested grids that allow for the solution to be focused in areas of interest. Also, the results show that the MODFLOW-2005 simulation takes about 20 times longer to complete the run and uses about 6 times more cells number than the MODFLOW-USG simulation.

Keywords: MODFLOW 2005; MODFLOW-USG; PEST; Damietta branch; El-Manzala Lake; Eastern Nile Delta

Introduction

Population increase on a universal scale is forcing more stress on environmental resources, such as water resources. Over the century, the total population of Egypt increased from 11 million in 1907 to 90 million in 2015, according to the Central Agency for Public Mobilization and Statistics [1]. The major part of this increase was intensified in the Nile Delta area. It is very heavily populated, with population densities up to 1600 inhabitants per square kilometer [2], which exert profound pressure on natural resources of land and water. The Egyptian government has started plans to regulate this situation since the 1980s by redistributing the population by applying an efficient horizontal urban expansion along the desert areas and near the border of the Nile delta.

The complex nature of environmental problems and complex geological systems requires the use of mathematical models capable of simulating the flow of groundwater in these heterogeneous media [3]. Recently, groundwater flow models have become the most active and effective tools that help water resource planners develop water plans and depict management policies over time series with different scripts using transient simulations [4]. To get a possible accurate simulation, boundary conditions, hydraulic properties, initial conditions data and real field observation should be determined [3].

Mathematical models remain an important mechanism for understanding hydrogeological phenomena, defining aquifer parameters and obtaining a reasonable estimate of the hydrogeological behavior [5,6]. In 1988, United States Geological Survey (USGS) launch of MODFLOW software package [7]. MODFLOW is a well-known public domain, three dimensions, block cell-centered, finite difference, and saturated flow model. MODFLOW can proceed both steady-state and transient analyses and has a wide variety of boundary conditions and input options [6-10].

The standard MODFLOW releases are all based on a rectangular finite-difference grid. But there are two restrictions with a standard finite-difference grid. The first is that irregularly shaped domain boundaries cannot be easily fitted with a rectangular grid. In spite of there are choices for inactivating accessories of the grid outside the domain of interest, the domain is still bounded by rectangular grid cells that may not pursue irregular boundaries; accordingly, information about the entire grid, including inactive cells, is read and processed [11]. Another limitation of a rectangular finite-difference grid is that it is severe to refine the grid resolution in areas of interest. Row and Column widths can be variably spaced so as to concentrate grid resolution, but the added resolution must be executed to the borders of the grid [11].

Since 2013 the authorized version of MODFLOW-USG with Unstructured Grid software package appeared on USGS website which represents a new approach in mathematical modeling of groundwater. MODFLOW-USG is based on a dependent control volume finite difference (CVFD) formulation in which a cell can be connected to an arbitrary number of closed cells. The new MODFLOW-USG program will eliminate most of the limitations in traditional MODFLOW. MODFLOW-USG was developed to support a wide assortment of structured and unstructured grid types, including grids based on

Citation: Ezzeldin MM, El-Alfy KS, Abdel-Gawad HA, Abd-Elmaboud EM (2018) Comparison between Structured and Unstructured MODFLOW for Simulating Groundwater Flow in Three-Dimensional Multilayer Quaternary Aquifer of East Nile Delta, Egypt. Hydrol Current Res 9: 297. doi:10.4172/2157-7587.1000297

prismatic triangles, rectangles, hexagons, and other cell formats. Elasticity in grid design can be used to concentrate resolution along, for example, rivers and around wells or to sub-discretize individual layers to better represent hydro-stratigraphic units [11].

In the present study, the major objective is to build a multilayer three-dimensional groundwater flow model to East Nile Delta aquifer based on the overall conceptual comprehension of the aquifer system and the available well data using MODFLOW 2005 and MODFLOW USG. Also, this study presented the basic advantages of MODFLOW USG software package that tends to set new criteria in groundwater modeling.

Site Description

The area of study located in the northeastern part of the Nile Delta and is bounded by the Mediterranean Sea and El Manzala Lake to the north, to the east by the Suez Canal, to the west by the Damietta Branch of Nile River and to the south by the Cairo-Suez Desert Road. It is located between latitudes 30˚00′and 31˚30′N and longitudes 31˚00′and 32˚30′E (Figure 1a and 1b). The topography of the northeastern Nile Delta is characterized by a low relief, and its surface slopes gently towards the northerly direction, while it holds a rolling shape towards the south, where the ground climbs up to a moderately elevated plateau with elevations that range between 2 m and 24 m above sea level (Figure 1b). Mean yearly rainfall ranges between 20 and 100 mm [12,13]. The main surface features in the survey area are active and fallow agricultural areas, urban shopping malls, sandy desert, freshwater canals, saltwater bodies, and marshland [14].

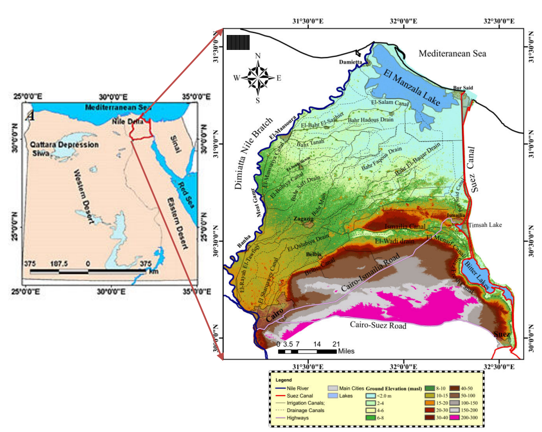

Figure 1: a) Map of Egypt, and b) Location map and digital elevation model of the Eastern Nile Delta region, Egypt.

Generally, the geological study in the area east of Nile Delta during Neogene- Quaternary times are discussed by many workers [15-18]. These studies concluded that the Eastern Nile Delta region was continuously and rapidly changing in deposition conditions. As well sedimentation of the Nile delta has been affected by many natural factors, including sea level fluctuations, fluvial, tectonic stability climatic and marine processes as well as drainage basins, which received water and sediments. At the topographic features in the southern part of the study area faulting is obviously noted which was covered by Miocene sediment folding that may show local imprint. These faults were begun during the Oligocene and repeated at later times [19]. The fractures basaltic lava infiltrated to overlie the Oligocene gravels and sands along these faults and underlies the Miocene marine sediments [20].

The sedimentary succession is dominated from top to bottom by the Nile silt, followed by the old deltaic sands and gravels which are underlain by fluvio-marine deposits forming the Quaternary aquifer (Figure 2a). These sediments can be based on the impervious pyritic clay and gypseous marls, especially in the vicinity of Damietta branch. However, in the most eastern parts, the basal portion of the deltaic deposits rests unconformable on a thick marine clay section, which belongs to Pliocene and Miocene.

The thickness of the studied aquifer of the eastern Nile delta increases toward the sea attaining 900 m thick close to the sea and gradually reduction southward to 100 m thick (Figure 2b) [21,22]. In the east of the cultivated area of Damietta branch topped the aquifer layer of silty clay which displays semi-confined conditions. In the remaining area, the formation of the water carrier is exposed to the surface and groundwater occurs under unconfined conditions. The body of the groundwater in the study area forms the eastern limbs of the huge convex lenses that occupy the entire delta region. Freshwater is directly related to the body of the water-bearing classes. Its thickness generally decreases north and east due to saltwater intrusion. A fresh column of fresh groundwater of about 300 meters was observed near Damietta branch in the south. While in the north the thickness of the freshwater body is gradually decreasing towards high salinity areas [23].

The Quaternary aquifer in eastern Nile Delta is mainly recharged by downward vertical infiltration of water from Damietta branch, Ismailia Canal and seepage from the network of irrigation canals and drains. The seasonal rainfall represents the minimal infiltration rate. The discharge occurs by pumping wells that used for the irrigation and domestic uses and by seepage into the Mediterranean Sea and Manzala Lake. There is upward and downward vertical motion between both shallow (phreatic water with clay cap) and the Nile Delta aquifer deeper water according to the difference between the piezometric head in the aquifer and the levels of the water table in the clay cap [22].

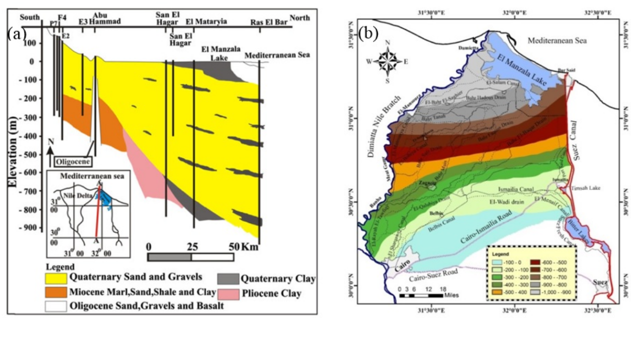

Figure 2: (a) Cross-section from south to north (El-Fayoumi) and (b) Isopach map of the thickness (meters) of the Quaternary aquifer in the East Nile Delta.

Material and Methods

In the present study, a three-dimensional finite difference and finite volume models were used to simulate groundwater flow in the Quaternary Aquifer East Nile Delta. MODFLOW-2005 and

Citation: Ezzeldin MM, El-Alfy KS, Abdel-Gawad HA, Abd-Elmaboud EM (2018) Comparison between Structured and Unstructured MODFLOW for Simulating Groundwater Flow in Three-Dimensional Multilayer Quaternary Aquifer of East Nile Delta, Egypt. Hydrol Current Res 9: 297. doi:10.4172/2157-7587.1000297

MODFLOW-USG were selected to numerically solve the governing flow equation based on water balance with a fully implicit finite difference approximation and dependent control volume finite difference (CVFD) formulation respectively [11,24]. The governing equation is written as follows [4,11].

$$\frac{\partial}{\partial x}\left(K_{xx}\frac{\partial h}{\partial x}\right)+\frac{\partial}{\partial y}\left(K_{yy}\frac{\partial h}{\partial y}\right)+\frac{\partial}{\partial z}\left(K_{zz}\frac{\partial h}{\partial z}\right)-\omega=S_S\frac{\partial h}{\partial t}$$

Where K_{xx}, K_{yy}, and K_{zz} are hydraulic conductivity values (in meters per day) along x, y, and z axis; h is the hydraulic head (in meters); ω is a source and sink term (volumetric flux per unit volume per day); S_S is the specific storage (per meter^{-1}); and t is time (in days). All calculations and modeling processes were carried out using Groundwater Modeling System (GMS 10.2) software [25].

Building the three-dimensional stratigraphic model

Complex stratigraphy is usually difficult to simulate in the traditional MODFLOW models as MODFLOW-2005 uses a structured grid, requiring that each grid layer be consistently continuous throughout the model domain [4]. On the other hand, the layers in MODFLOW-USG do not need to be continuous but it is possible to simulate faults and discontinued layers thus considerably beneficent the conceptual model of the treated aquifer. A CVFD method performed on the MODFLOW USG software package strengthens the flexibility of grid element's geometry, field dimensions and elements that can facilely be modified and customized [11].

The following represents the typical steps applied in construction of three-dimensional models from borehole data.

Importing borehole data: The lithology of the 390-borehole data and related hydraulic conductivity and other hydraulic parameters were collected from literature. Figure 3 shows the location of the boreholes data set in the study area, colors symbolize the surface lithology. Six hydro-stratigraphic units were defined in the Quaternary aquifer including clay, sandy clay, fine sand, coarse sand, limestone and sand and gravel as shown in Figure 4.

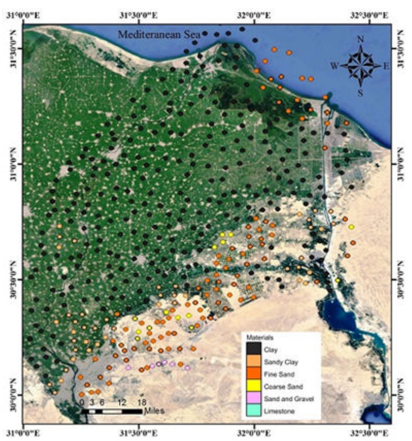

Figure 3: Locations of the boreholes data set in the study area illustrative on the satellite image of 2017.

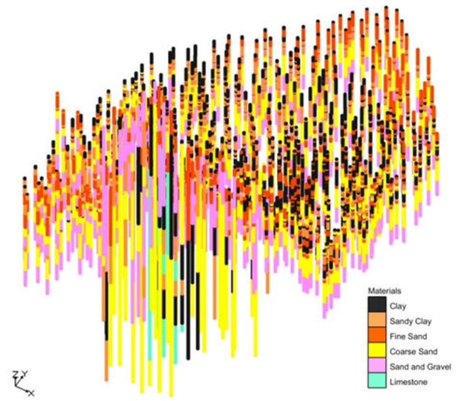

Figure 4: Three-dimensional view of the study area 390 borehole data with their lithological succession. The yaxis follows the north direction; Figure is not to scale.

Assigning horizon IDs: The horizon points out to the top of each hydro-stratigraphic unit. Horizon IDs were automatically assigned for each borehole, in the order that the units were deposited at the stratigraphic contacts from bottom to top [6]. Thirty horizons were specified in the borehole data from the six hydrostratigraphic units. Figure 4 displays a three-dimensional view of the borehole data after horizon IDs specification. Then polylines and polygons of borehole cross sections that define the stratigraphy between two boreholes were automatically created by using a triangulation process to set the most probable connections between boreholes.

TIN construction and creating solids: TIN was built in the map module of the GMS 10.2 to determine the boundary of the solids and generate the horizons surfaces. Then the digital elevation model (DEM) of the study area was imported and interpolated to the TIN. Borehole cross sections then were used to create solids using Natural Neighbor interpolation method.

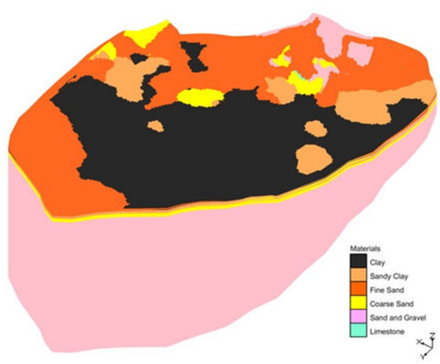

Figure 5: 3D views of the solids created from 3D borehole data of the study area.

The top elevation of the solids was automatically assigned using the ground level data from the DEM and the bottom elevation was assigned using the isopach map of the thickness of the Quaternary aquifer in the Eastern Nile Delta as shown in Figure 2b. A grid layers were assigned to the solids in which the layer ranges were set to map

Citation: Ezzeldin MM, El-Alfy KS, Abdel-Gawad HA, Abd-Elmaboud EM (2018) Comparison between Structured and Unstructured MODFLOW for Simulating Groundwater Flow in Three-Dimensional Multilayer Quaternary Aquifer of East Nile Delta, Egypt. Hydrol Current Res 9: 297. doi:10.4172/2157-7587.1000297

each horizon in the solids to a single layer in the MODFLOW grid. The resulting solids and cross sections cut through the developed solids of the Eastern Nile Delta aquifer are shown in Figures 5 and 6 respectively.

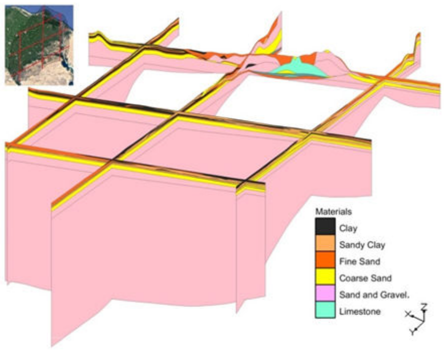

Figure 6: Cross sections showing the complex distribution of the different units in the study area.

Structured and unstructured grid generation: Structured MODFLOW uses a straight line finite difference grid consists of a group of columns, rows, and layers. Rectangular shaped cells that often make it difficult to form a grid into complex layers and features. Also, structured MODFLOW must have a model domain in the form of a rectangle. The cells outside the area of utility must be set as inactive so as to accommodate irregularly shaped model domains, as shown in Figure 7.

MODFLOW 2005 solves the groundwater flow equation in a cell by cell basis in the 3D grid, where the unit elevation arrays and equivalent hydraulic properties are assigned to each cell. Solids models are very beneficial in providing the finite difference grid of MODFLOW with layer elevation arrays and hydro-stratigraphic information. This information is automatically inherited from the constructed solids on a cell by cell basis to MODFLOW grid [6].

Before convert solids to traditional MODFLOW, a 3D finite difference grid of 175 columns, 250 rows, and 30 layers were constructed and rotated 17˚ from north direction, so that the MODFLOW grid is parallel to the predominant direction of groundwater flow. Overall dimensions of the model in x, y and z directions are 105000, 150000 and 1230 meters, respectively. Subsequent to grid construction, MODFLOW was initialized and the starting head was set to a constant value of 20 m above the mean sea level. The solids were finally interpolated to a MODFLOW grid using the boundary matching algorithm to compute a set of elevation arrays that honor the boundaries between the stratigraphic units as closely as possible. Figures 8 and 9 show the MODFLOW 3D grid after interpolating the solid data on a cell by cell basis in the 3D structured grid. As shown in Figure 9, with structured MODFLOW, model layers should be continuous across the entire model domain; this makes it difficult to create intermittent formations within the model or a small formation within a larger aquifer. To conciliate this, an entire model layer must be integrated, with a minimum layer thickness defined in the pitchout regions. Typically, the parameter values of these very thin cells are assigned from the formation above or below for continuity. In addition, the number of cells must be the same in all model layers with structured MODFLOW; this is inactive because it means that a large number of cells in layers above or below the area of interest will be generated [26].

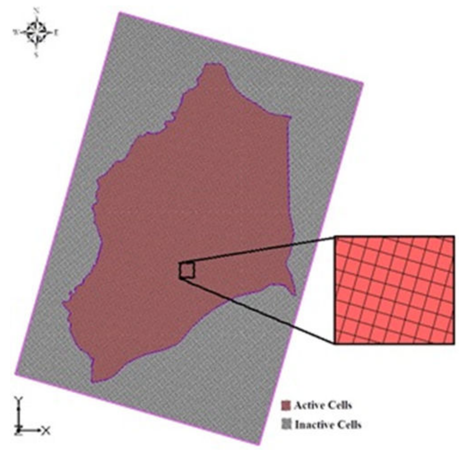

Figure 7: Plan views of the study area show rectangular grids of structure MODFLOW.

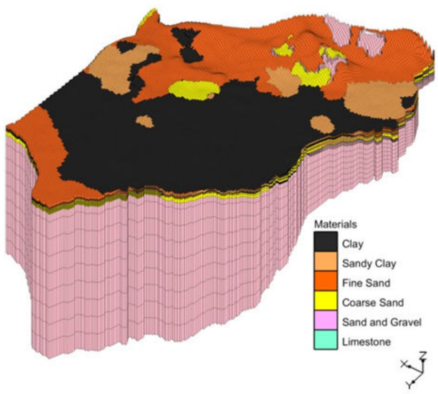

Figure 8: 3D views of the structured grid solid consist of 175 column, 250 rows, 826110 cells and 30 layers.

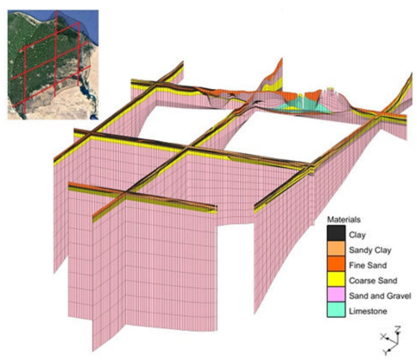

Figure 9: Cross sections showing continuous of model layers across the entire model domain.

Citation: Ezzeldin MM, El-Alfy KS, Abdel-Gawad HA, Abd-Elmaboud EM (2018) Comparison between Structured and Unstructured MODFLOW for Simulating Groundwater Flow in Three-Dimensional Multilayer Quaternary Aquifer of East Nile Delta, Egypt. Hydrol Current Res 9: 297. doi:10.4172/2157-7587.1000297

On the other hand, MODFLOW-USG utilizes a finite volume formula, which supplies the cell geometry with greater elasticity. The grid cells can be created with any shape: rectangles, triangles, polygons, hexagons, etc. In this study Voronoi polygons is used (Figure 10), as this grid geometry accommodating complex stratigraphy and also provides a great level of flexibility for refining the grid around model features. Voronoi polygon cells supplying higher reliability and better model convergence than rectangular cells. With MODFLOW-USG, cells are specified by a Node ID. Cells are numbered beginning from the top layers to the lower layers.

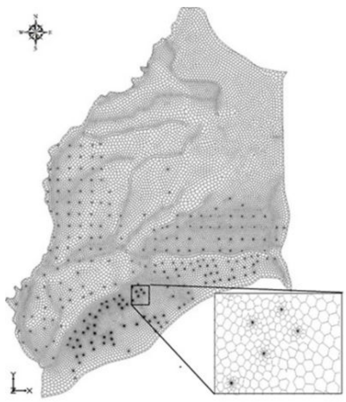

Figure 10: Plan views of the study area show grids of Unstructured MODFLOW.

Counter to the traditional MODFLOW, MODFLOW-USG allows the definition of model fields irregularly. As a consequence of this, there are no inactive cells established in those areas outside of interest, this is illustrated in Figure 10. With MODFLOW-USG, only to the areas of interest, the grid can be refined. The grid can be locally-refine around a line or polygon features and good features that represent boundary conditions. Cells with smaller cell size are found in the areas of interest (resulting in higher accuracy), while outside the area of interest fewer cells with larger cell size can be maintained [26].

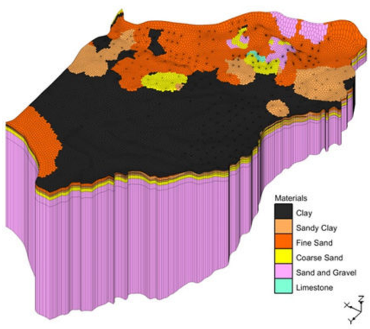

Figure 11: 3D views of the unstructured grid solid consist of 193899 cells and 30 layers.

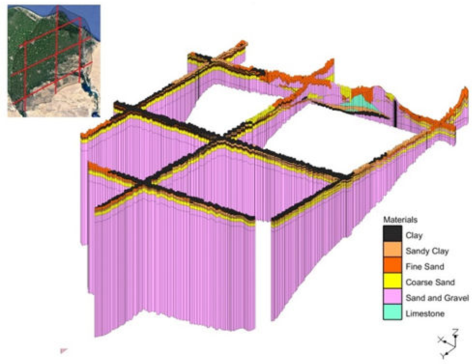

Figure 12: Cross sections showing non-continuation of model layers across the entire model domain.

Layers with MODFLOW-USG are not continuous across the total model domain, this means that layers can pinch out to zero thickness as shown in Figures 11 and 12. Also, with MODFLOW-USG, each layer can include its own discretization; based on that refine of the grid can be around rivers and streams in the upper layers and have rough refinement in lower layers. Finally, the result with MODFLOW-USG is quicker solutions, fewer cells, with maintaining high accuracy.

Developing GIS-based conceptual model

In conceptual models, all model parameters are prepared as boundary conditions, sources and sinks, and observation points [4]. Building the conceptual model of the study area included the following procedures.

Importing background digital images and maps: Firstly, the satellite image of 1990 was imported as a base map for the project steady state and georeferenced to the same coordinate system and projection. Then the satellite image of 2017 was imported also to determine the places of urban extension and reclaimed land.

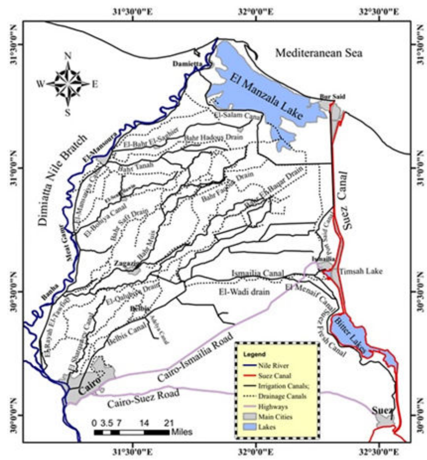

Figure 13: Surface water system in the study area.

Also, the surface water system map (Figure 13) was imported and converted to features (points, arcs, and polygons) using the GIS tools in the map module. All map features of the study area should be assigned in coverage set up for the individual coverage in the map module so that the input information for each feature can be identified when creating any feature object.

Building sources and sinks coverage: The sources and sinks coverage included the boundary conditions and all water budget components excepting recharge zones, which were mapped in a separate coverage. It is usually suitable to select natural boundaries such as a river, lake, and mountain ridge to delineate the model boundaries because they are usually stable features in the flow system. Damietta Branch in the west, Suez Canal in the east, the Mediterranean Sea in the north and Cairo-Ismailia Road on the south were selected to delineate the boundaries of the modeled area. First two boundaries were mapped as a Cauchy boundary condition (Fixed reference water level with additional transfer rate) using the information in Table 1. The other was mapped as Dirichlet boundary condition (Fixed hydraulic head).

Water Body	Total Length (Km)	Bottom width (m)	Mean Depth (m)	Range of Surface water level	Conductance (m^2/d)/(m) (Calculated)
Demietta branch	245	200.0:500.0	6.0	16.0:-1.0* m	0.03:0.12
El Rayah El Tawfiky	63	10.0:26.0	5.0	16.0:0.5 m	0.0075:0.05
Ismaelia Canal	136	10.0:30.0	5.0	16.0:0.0 m	0.0025:0.1
El Sharkaweya Canal	32	7.0:10.0	5.0	16.5:13.0 m	0.007:0.03
El Basoseya Canal	24	5.0:10.0	5.0	16.0:12.0 m	0.025:0.05
Bahr El Baqar Drain	85	100.0:200.0 m	5.0	-	0.05:0.2
Bahr Hadous Drain	50	5.0:40.0 m	5.0	-	0.01:0.1
El Serw Drain	30	5.0:10.0 m	5.0	-	0.025:0.05
Suez Canal	173	-	16.0	-	0.1:0.2
El Manzala Lake (area)	1500 Km^2	-	1.2	1.0:0.0 m	0.00012

Table 1: The main irrigation canals, drains and lakes in the study area [29]. Note: this value is not logical, so these values are excluded in this study.

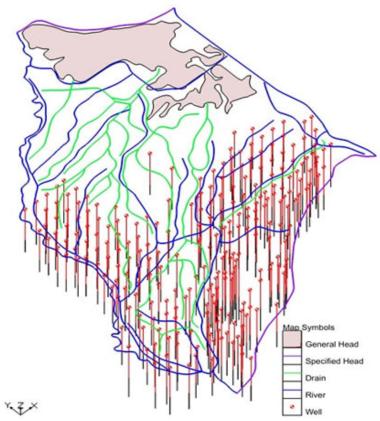

Figure 14: The y-axis follows the north direction; Figure is not to scale.

Figure 14 shows 3D view of all conceptual model elements. El Manzala Lake was simulated as a general head polygon with a general head of 0.50 m amsl, where the inflow/outflow across the boundary is computed by Q_B=*Conductance**(h_{out}-h_{aquif}), where h_{out} is a specified head outside the domain, h_{aquif} is the unknown (simulated) head next to the boundary inside the aquifer and conductance (m^2/d) is the conductance of the soil in the boundary segment [7]. Irrigation canals and drains (Figure 15) were mapped as a Cauchy boundary condition using the river and drain package of MODFLOW, respectively. In the case of a Cauchy boundary condition, conductance is the main input parameter in most sources and sinks features. Conductance point out to the vertical movement of water through soil and is defined in MODFLOW as the hydraulic conductivity of the river bed materials divided by the vertical thickness of the river bed materials, multiplied by the area (width times the length) of the river in the cell [7]. Water may flux into or out of the aquifer building on the head difference between the aquifer and the source or sink feature. Length and width of each river sections are required to define the conductance term. In case of drains, conductance term acts only as a sink for water, so if the drain bottom elevation is higher than the calculated groundwater head the leakage is automatically set to zero. The head and riverbed conductance were assigned based on Table 2 and missing data estimated relative to the nearest known head.

A pumping well is considered a point sink and is represented in the model by a node. In finite difference and finite volume models the node represents cell and so the gradient induced by the pumping effect cannot be expected. Consequently, the head calculated by the model is not needs symbolizing the groundwater head in the well, but on going away from the well node the computed head is correct.

There are no data on the current levels of groundwater extraction in the Nile Delta. Contradictions related to the total irrigated area with groundwater can be observed in published data [26]. The east Nile Delta aquifer serves six governorates, and according to the FAO report

Citation: Ezzeldin MM, El-Alfy KS, Abdel-Gawad HA, Abd-Elmaboud EM (2018) Comparison between Structured and Unstructured MODFLOW for Simulating Groundwater Flow in Three-Dimensional Multilayer Quaternary Aquifer of East Nile Delta, Egypt. Hydrol Current Res 9: 297. doi:10.4172/2157-7587.1000297

(2013) the total irrigated area using groundwater is 51055 feddan (888 feddan in Daqahleya, 11738 feddan in Qalyoubeia, 11290 feddan in Sharkeya, 7139 feddan in Ismailiya, and no land areas is being irrigated with groundwater in Damietta, and Port Said due to the impact of saltwater intrusion from the Mediterranean Sea in those governorates. In this study, 240 sites were selected to represent more than 7400 production wells that pumped a total volume of approximately 2.5 million m^3/d during 1990 from the study area [6] and 3.4 million m^3/d during 2004 [27]. The spatial distribution and the pumping rate of each well site were set from the hydrogeological map of Egypt-1992, and data published in the literature review as shown in Figure 14. In all wells, screen intervals were assigned based on the pumping rate and well depth and high-intensity fluxes were assigned to the low sand and gravel unit to avoid dry cells effect [6].

Planning recharge zones coverage: Recharge refers to the volume of the infiltrated water (from excess irrigation water and seepage from the river branches, canals and drainage systems due to the thinner clay layer) that becomes a part of the groundwater flow. Groundwater flow modelers have traditionally assumed spatially uniform charge rate and often adjust it during model calibration [28].

Recent studies included various recharge zones were delineated from the satellite images of 1991, 2005 and 2015 to map the initial steady state model for the year of 1991 and thereafter represent the increase in agricultural development through the 1991-2015 for the transient simulation. At least 40 recharge zones were specified in the agricultural land and for calibration, the initial recharge rates ranged between 0.00000127 m/d to 0.00006 m/d in the traditional agricultural land and 0.00006 m/d to 0.00102 m/d in the newly reclaimed land.

Also, evapotranspiration has important impacts on recharge rate and groundwater quality, especially in regions that fall in the semi-arid zone [6]. El Haddad showed that evaporation rates decrease towards the north and east with the low value recorded in El Zagazig 102 mm/yr and a high rate in Suez 140 mm/yr [29].

Results

Steady state calibration

Before the first run of the model the model was specified as convertible conditions confined or unconfined based on the hydraulic conductivity value disparity of the model layers [30]. Then the simulation was examined for errors and warnings using the check simulation command in structure and unstructured 3D grid module to assure model conversion and accurate solution. After the first succeeded run in the steady state, the model calibration by combining the forward MODFLOW model with the computer-based program PEST (which is an acronym for Parameter ESTimation) to adjust the input parameters until the calculated and observed head in observation points reach passable agree. In the present study, recharge and the hydraulic conductivity are assumed unknown flow parameters. Though hydraulic conductivity and recharge are both spatially variable, zonation as a parameterization technique is adopted to transform its spatial variability to uniform values zones. The accommodation of any inversion model depends on the careful choice and application of optimization algorithms. Parameter inversion methods are most usually carried out using gradient-based methods such as Levenberg Marquardt technique [31]. This study used PEST to accomplish this task.

The computer-based program PEST was firstly progressive by Doherty and has been extensively used in hydrologic modeling [32]. Besides its strong ability on model calibration with mathematical regularizations depending on Gauss-Marquardt-Levenberg method and the help of a parameterized inverse approach, the PEST software efficiency is raised by its complementary implementations of predictive error and uncertainty analysis as well as stochastic simulation utilities [33-35]. The standard used to stop execution by PEST include a two reasonable termination, which is either optimal parameter has been calibrated or additional execution will not continue in diminishing objective function. To achieve such a performance, a number of different gauge are compiled in PEST. Foremost, value of objective function is said to stop execution with three factors, which are max number of relative convergence iteration (NPHISTP), relative convergence limit (PHIREDSTP) and max number of iteration with no improvement (NPHINORED). If the relative convergence changes less than PHIREDSTP over NPHISTP successive iterations, or the execution to reduce the objective function over NPHINORED successive iterations, the optimization process will be stop. Also, parameter change is another index that PEST desires no more iteration. The PEST commands unlikely to achieve a better result if the maximum parameter change during the last Max Number of Parameter Change Iterations (NRELPAR) is less or equal to Relative Parameter Change Criterion (RELPARSTP). Finally, the value of Max Number of Iterations (NOPTMAX) should not be the reason that parameter estimation ceases to be executed, so optimization of the parameter set is guaranteed [35]. The values of calibration termination control factor used in this study are shown in Table 2.

In this study, the number of parameters being estimated is 55 parameters, consisting of 30 hydraulic conductivity zones and 25 recharge zones. The number of observations well in 1991 is 73. For both Structure and Unstructured grid, PEST stop execution when 3 optimization iterations have elapsed since lowest objective function was achieved. To complete parameter estimation structure grid model needed 18 iterations and 55.12 hour, but unstructured grid needed 8 iterations and 10.48 hour.

Control	Full name	Value
NOPTMAX	Max Number of Iterations	50
NPHINORED	Max Number of Iterations with No Improvement	5
PHIREDSTP	Relative Convergence Limit	0.005
NPHISTP	Max Number of Relative Convergence Iteration	5
RELPARSTP	Relative Parameter Change Criterion	0.005
NRELPAR	Max Number of Parameter Change Iterations	5

Table 2: Values of calibration termination control factors.

The final hydraulic conductivity for structure and unstructured grids that were used in the calibrated steady-state model are displayed in Table 3.

Model layers	Lithology	Level (m)		Hydraulic conductivity (m/day)				Specific yield	Specific storage (m^{-1})
		Max	Min	Structure grid		Unstructured grid			
				Horizontal	Vertical	Horizontal	Vertical		
1	Upper Clay	80.96	-24.8	0.006	0.0012	0.0045	0.0009	0.05	0.08
2	Sand Clay	58.0	-25.14	0.765	0.153	0.82	0.164	0.06	0.001
3	Fine Sand	231.7	-38.7	1.32	0.264	1.28	0.256	0.25	0.005
4	Coarse Sand	188.8	-54.5	45.8	9.2	42.85	8.57	0.3	0.0004
5	Clay	223.0	-66.4	0.0045	0.0009	0.006	0.0012	0.05	0.08
6	Sandy Clay	172.7	-63.1	1.02	0.204	0.69	0.138	0.06	0.001
7	Fin Sand	187.9	-61.9	1.32	0.264	2.26	0.452	0.25	0.005
8	Clay	75.8	-43.1	0.003	0.0006	0.0014	0.00028	0.05	0.08
9	Coarse Sand	171.2	-63.1	62.5	12.5	66.18	13.236	0.3	0.0004
10	Clay	26.1	-40.2	0.006	0.0012	0.001	0.0002	0.05	0.08
11	Sandy Clay	72.8	43.1	1.02	0.204	0.88	0.176	0.06	0.001
12	Fine Sand	168.13	-43.1	1.32	0.264	1.2	0.24	0.25	0.005
13	Coarse Sand	166.1	-43.1	65	13.4	67.5	13.1	0.3	0.0004
14	Sand and Gravel	233.8	-70.1	92.6	30.68	89.58	29.86	0.35	0.00004
15	Fine Sand	38.1	-34.1	1.32	0.264	1.18	0.236	0.25	0.005
16	Clay	142.3	-69.3	0.002	0.0004	0.0016	0.00032	0.05	0.08
17	Sandy Clay	179.8	-61.9	0.765	0.153	0.64	0.128	0.06	0.001
18	Coarse Sand	206.9	-69.7	66.46	13.292	70.0	14.0	0.3	0.0004
19	Sand and Gravel	110.1	-76.7	122.56	24.512	125.0	25.0	0.35	0.00004
20	Limestone	91.0	-75.2	6	1.2	5.20	1.04	0.18	1.0e-6
21	Sandy Clay	88.5	-80.0	1.02	0.204	1.27	0.254	0.06	0.001
22	Coarse Sand	67.1	-74.9	76.5	15.3	80.86	16.172	0.3	0.0004
23	Sandy Clay	32.8	-87.7	1.02	0.204	0.64	0.128	0.06	0.001
24	Limestone	0.80	-86.4	6	1.2	5.0	1	0.18	1.0e-6
25	Sandy Clay	-25.8	-88.9	1.02	0.204	0.75	0.15	0.06	0.001
26	Fine Sand	30.3	-81.6	1.32	0.264	1.15	0.23	0.25	0.005
27	Clay	-17.9	-100.0	0.006	0.0012	0.0012	0.00024	0.06	7.0e-7
28	Coarse Sand	26.9	-100.0	85.0	17.0	85.0	17.0	0.3	0.0004
29-30	Sand and Gravel	4.8	-1000.0	150.0	50.0	130	45.0	0.35	0.00004

Table 3: The hydraulic parameters for the different 30 layers in Quaternary Aquifer East Nile Delta area.

To compare different models, some factors are defined such as Mean Absolute Error (MAE), Root Mean Square Error (RMSE), correlation coefficient (R), and Mean Relative Error (MRE). The Comparison of statistical parameters for assessing the calibration of the steady-state model between the structured grid and the unstructured grid is shown in Table 4. The results shown in Table 4 indicate a somewhat better of the unstructured grid than the structured grid.

The simulated head distribution in the eastern Nile Delta aquifer as calculated from the calibrated steady state that represents the

Citation: Ezzeldin MM, El-Alfy KS, Abdel-Gawad HA, Abd-Elmaboud EM (2018) Comparison between Structured and Unstructured MODFLOW for Simulating Groundwater Flow in Three-Dimensional Multilayer Quaternary Aquifer of East Nile Delta, Egypt. Hydrol Current Res 9: 297. doi:10.4172/2157-7587.1000297

conditions of the aquifer system in 1990 for the structured and unstructured grid is shown in Figure 15. Also, the calibration index bars of 73 observation wells are presented in this Figures that displays good calibration (a green bar points out less than 0.5 m difference between observed and calculated groundwater head) throughout the area, but the southern part of the modeled area had some intermediate calibration (a yellow bar points out 0.5-1.0 m difference in groundwater head). Figure 16 present the plot of the calculated and observed head values for all observation points used in model calibration.

Statistical parameters	Structured grid	Unstructured grid
MAE	0.256	0.216
RMSE	0.311	0.249
R	0.9967	0.9972
MRE%	5.705%	4.433%

Table 4: The statistical parameters for assessing the calibration of the steady-state model.

A comparison between MODFLOW-2005 and MODFLOW-USG for the eastern Nile Delta aquifer simulations shows some of the advantages of using the unstructured grid approach to this special problem. Plots of simulated groundwater head for 1991 show similar head patterns for the two different models (Figure 15). Results from MODFLOW-USG are more refined than the results from MODFLOW-2005 especially along rivers, drains, the coastline, and within the well fields. A comparison of the cumulative water budget for the steady-state simulation period 1991 is shown in Figure 17. As shown in this figure, there are some slight differences in the individual water budget components between the two models. The largest percent difference is for recharge, rivers and drains leakage into the model. MODFLOW-2005 simulates a cumulative rivers leakage value that is about 2.16% greater than the value simulated by MODFLOW-USG. MODFLOW-USG simulates a cumulative recharge and drains leakage value that is about 2.42% and 0.8% greater than the value simulated by MODFLOW-2005, respectively.

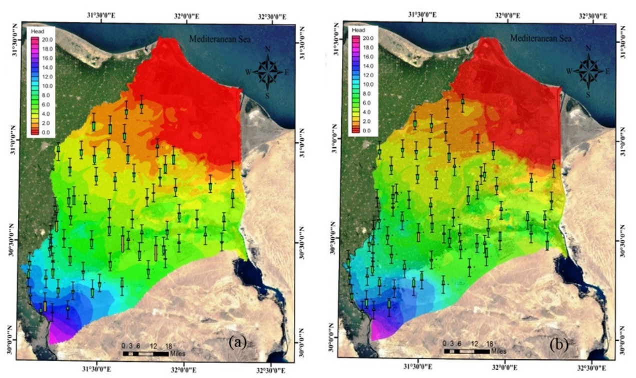

Figure 15: Simulated head values in 1991 using a) MODFLOW-2005 and b) MODFLOW-USG.

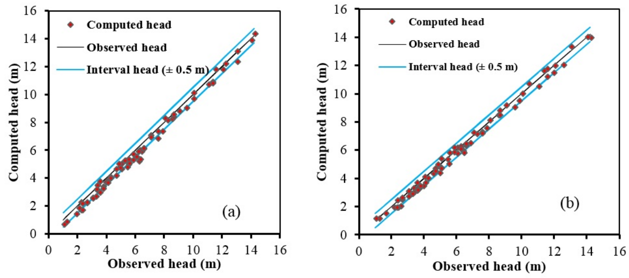

Figure 16: The statistical plot to the observed and calculated head for the observation wells resulted from a) structured grid and b) unstructured grid.

Table 5 listed various serious differences between the MODFLOW-2005 and MODFLOW-USG simulations. The MODFLOW-2005 simulation takes about 20 times longer to complete the run and uses about 6 times more cells than the MODFLOW-USG simulation.

Simulation characteristic	Structured grid	Unstructured grid
Number of cells	1312500	235893
Runtime Steady state (s)	751.55	34.771
Runtime transient state (s)	15600	854.5
Computer memory (kilobytes)	308	28

Table 5: Summary of differences between the MODFLOW-USG and MODFLOW-2005 simulation for the study area aquifer in steady state.

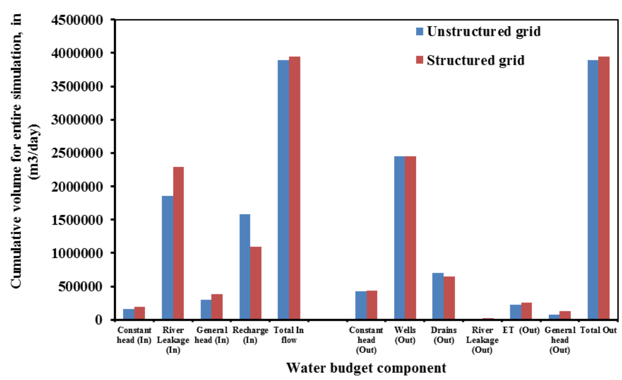

Figure 17: Cumulative water budgets for the simulation of the Eastern Nile Delta aquifer in 1991.

Transient state model

After calibrating model in the steady state, transient simulations are generally recommended to resolve time-dependent hydrogeological problems. In the present transient simulation, most of the input parameters of the calibrated steady model were utilized. The specific yield and specific storage characteristics of hydro-stratigraphic units were adjusted using the data in Table 3. Taking into account the

Citation: Ezzeldin MM, El-Alfy KS, Abdel-Gawad HA, Abd-Elmaboud EM (2018) Comparison between Structured and Unstructured MODFLOW for Simulating Groundwater Flow in Three-Dimensional Multilayer Quaternary Aquifer of East Nile Delta, Egypt. Hydrol Current Res 9: 297. doi:10.4172/2157-7587.1000297

possible ranges of specific yield and specific storage values published in the literature. The 128 head data of 2004 collected from literature [6,18] with 0.5 m head interval were used as an observed transient head. For the transient calibrations, the model was run from the year 1991 to 2004, using the head results of the optimal steady-state 1991 calibration run as starting heads. The transient model was considered calibrated and represents the hydro-geological setting in east Nile Delta aquifer on 2004 when the variation between the calculated and observed heads was minimized.

Statistical parameters	Structured grid	Unstructured grid
MAE	0.253	0.169
RMSE	0.328	0.22
R	0.995	0.998
MRE%	4.964	3.157

Table 6: The statistical parameters for assessment the calibration of transient model.

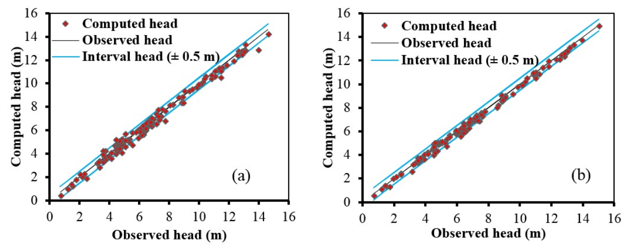

Figure 18: A statistical plot to the observed and calculated head for the observation wells in 2004 resulted from a) structured grid and b) unstructured grid.

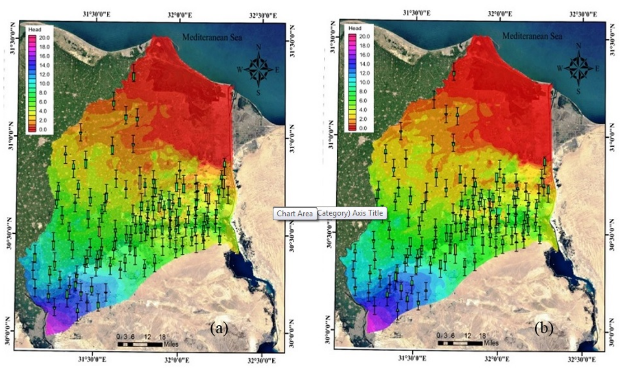

Figure 19: Simulated head values in 2004 using a) MODFLOW-2005 and b) MODFLOW-USG.

The values of statistical parameters of the transient calibration (MAE, RMSE, R, and MRE %) are shown in Table 6. Figure 18 show a plot of calculated and the observed head value of 125 observation points for the structured and unstructured grid. In general, a good correspondence between observed and calculated values for all areas was found. The simulated head distribution in the eastern Nile Delta aquifer as calculated from the calibrated transient state that represents the conditions of the aquifer system in 2004 for the structured and unstructured grid is shown in Figure 19.

Model verification

Model verification used to check whether the calibrated model is capable to predict observed hydraulic heads for subsequent time periods not yet [36]. For verification, the heads measured in the year 2015 is used. As Figure 20 shows, a very good agreement between simulated and observed groundwater heads is also obtained for this year of verification. The values of statistical parameters of the model verification are shown in Table 7.

Statistical parameters	Structured grid	Unstructured grid
MAE	0.300	0.208
RMSE	0.362	0.256
R	0.985	0.999
MRE%	9.56	6.06

Table 7: The statistical parameters for assessment the model verification.

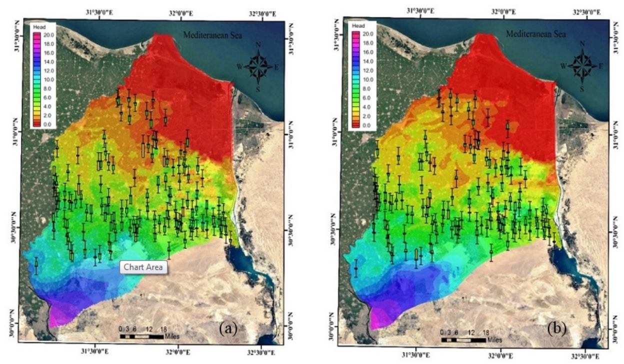

Figure 20: Simulated head values in 2015 using a) MODFLOW-2005 and b) MODFLOW-USG.

Figure 21 show the absolute differences of inflow and outflow groundwater budgets between Modflow-2005 and Modflow-USG calculated from the transient simulation between 1991 and 2015. In examining Figure 21a, it is obvious that recharge and rivers leakage are the major differences in the inflow budget, but the constant head, general head, and storage are the minor differences. For the differences in the outflow water budget, discharge to drains formed the major differences.

These differences in groundwater budgets may be due to variations in the method of solution between finite difference method and finite volume method. The method of finite difference discretization is based on the differential form of the partial differential equation to be solved and finite volume method discretization is based upon an integral form of the partial differential equation to be solved. In the finite volume method, it is converted volume integrals in a partial differential equation containing the term spacing to surface integrals, using the theory of divergence. These terms are then estimated as fluxes on the

Citation: Ezzeldin MM, El-Alfy KS, Abdel-Gawad HA, Abd-Elmaboud EM (2018) Comparison between Structured and Unstructured MODFLOW for Simulating Groundwater Flow in Three-Dimensional Multilayer Quaternary Aquifer of East Nile Delta, Egypt. Hydrol Current Res 9: 297. doi:10.4172/2157-7587.1000297

surfaces of each finite volume. Because the entry flow of a certain volume matches that leaving an adjacent volume, these methods are conservative [37].

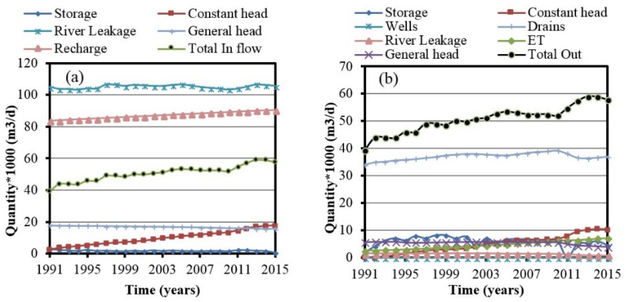

Figure 21: Plot of the absolute differences of a) inflow and b) outflow groundwater budgets between Modflow-2005 and Modflow-USG.

Conclusions

This study describes the advantages of using MODFLOW-USG, a new unstructured grid version of MODFLOW. This version is based on a control volume finite difference formulation that provides new flexibility in grid generation, including the ability to utilize nonrectangular cell shapes such as triangles, irregular polygons, and hexagons. The MODFLOW-USG can be applied to simple grids and also with nested grids that allow for results to be focused in areas of interest. The capabilities and features of the MODFLOW-USG program shows by work compared with MODFLOW-2005 which used the finite difference code to simulate groundwater head distribution throughout the aquifer system in the steady and transient state. For this, three-dimensional groundwater flow model was developed in the Quaternary aquifer eastern Nile Delta, Egypt. The stratigraphy of the aquifer was mapped to the 30 layer grid of MODFLOW from 390 borehole data using solid approach. In this study, rectangular cells and a Voronoi polygon are used for the structure and unstructured grid, respectively. Voronoi polygon cells supply a reliability and better model convergence than the rectangular cells. Counter to the MODFLOW-2005, MODFLOW-USG allows the definition of model fields irregularly, so there are no inactive cells established in those areas outside of interest. Also, layers with MODFLOW-USG should not be continuous across the total model domain; this means that layers can pinch out to zero thickness.

The steady state run was calibrated to the head data of the 1991 hydrogeological map of Egypt, the forward MODFLOW model is combined with the computer-based program PEST to adjust the input parameters until the calculated and observed head in observation points reaches passable matching. To complete parameter estimation structure grid model needed more 10 iterations and 44.16 hour than unstructured grid. These calibrated conditions were the initial conditions of the 1991-2004 transient simulation. The heads measured in the year 2015 was used for verification. The results of head simulation show similar head patterns for the two different models although MODFLOW-2005 simulation takes about 20 times longer to complete the run and uses about 6 times more cells than the MODFLOW-USG simulation. But results from MODFLOW-USG are more refined than the results from MODFLOW-2005 especially along rivers, drains, the coastline, and within the well fields. This led to small difference in the individual water budget components between the two models especially in recharge, rivers and drains leakage into the model. Also, this difference due to variations in the methods used for solution, the finite difference method against the finite volume method.

References

1. Central Agency for Mobilization and Statistics (2015) Population. Egypt Statistical Yearbook.
2. El-Ramady R, El-Marsafawy HR, El-Marsafawy SM, Lewis LN (2013) Sustainable agriculture and climate changes in Egypt. In Sustainable Agriculture Reviews pp. 41-95.
3. Pasquier P, Marcotte D (2006) Steady-and transient-state inversion in hydrogeology by successive flux estimation. Advances in Water Resources 29: 1934-1952.
4. Abdulaziz AM, Faid AM (2013) Evaluation of the groundwater resources potential of Siwa Oasis using three-dimensional multilayer groundwater flow model, Mersa Matruh Governorate, Egypt. Arabian Journal of Geosciences 8: 1-17.
5. Gaspar E (1987) Modern trends in tracer hydrology. CRC Press.
6. Ismael AM (2007) Applications of remote sensing, GIS and groundwater flow modeling in evaluating groundwater resources: Two case studies; East Nile Delta, Egypt and Gold Valley, California, USA. The University of Texas at El Paso.
7. McDonald MG, Harbaugh AW (1988) A modular three-dimensional finite-difference ground-water flow model. US Geological Survey Reston, VA.
8. Harbaugh AW (2005) MODFLOW-2005, the US Geological Survey modular ground-water model: the ground-water flow process. US Department of the Interior, US Geological Survey Reston, VA, USA.
9. Harbaugh AW (2000) MODFLOW-2000, The U. S. Geological Survey Modular Ground-Water Model-User Guide to Modularization Concepts and the Ground-Water Flow Process Open-file Report. U. S. Geological Survey, p: 134.
10. Harbaugh AW, McDonald MG (1996) Programmer's documentation for MODFLOW-96, an update to the US Geological Survey modular finite-difference ground-water flow model.
11. Panday S (2013) MODFLOW-USG version 1: An unstructured grid version of MODFLOW for simulating groundwater flow and tightly coupled processes using a control volume finite-difference formulation.
12. Elewa HH (2013) Determining groundwater protection zones for the Quaternary aquifer of northeastern Nile Delta using GIS-based vulnerability mapping. Environmental Earth Sciences 68: 313-331.
13. Zaid SM (2006) Geo-environmental study of Eastern Nile Delta, Egypt. PhD Thesis. Faculty of Science, Zagazig University, Egypt, p: 339.
14. Ezzeldin MM (2016) Land Use Changes in the Eastern Nile Delta Region; Egypt Using Multi-temporal Remote Sensing Techniques 7: 78-98.
15. Zaghloul MGED (1958) Flow Distribution Through the Ground Water Aquifer of the Nile Delta.
16. El-Fayoumi IF (1968) Geology of groundwater supplies in the Eastern region of the Nile Delta and its extension in the North Sinai. PhD Thesis, Faculty of Science, Cairo University.
17. El-Dairy MD (1980) Hydrogeological studies on the eastern part of the Nile Delta using isotope techniques. A Master Thesis submitted to Zagazig University, Egypt.
18. Abd El Hamid AT, El Mahmoudi AS, El-Haddad UAEIM (2005) Geoelectrical exploration for groundwater around the new communities, east nile delta, in 18th EEGS Symposium on the Application of Geophysics to Engineering and Environmental Problems.
19. El-Shazly EM, Shehata WM, Someida MA (1982) Hydrogeology of Inshas site. Egypt J Geol 26: 53-70.
20. Shukri NM, El Ayouty MK (1956) The geology of Gebel Iweibid-Gafra area, Cairo-Suez District. Bull Soc Geogr, Egypt 29: 67-109.

21. Shatta AA (1979) Soil map of the Eastern Delta Region, El Tumilat-Suez. 4th report. Internal report, Academy of Scientific Research Technology, Cairo, Egypt, pp: 89-105.

22. Abo-El-Fadl MM (2013) Possibilities of Groundwater Pollution in Some Areas, East of Nile Delta, Egypt. International Journal of Environment 1: 1-21.

23. Tantawi MA (1998) Hydrogeochemical and isotopic assessment of the Quaternary aquifer in the Eastern Nile Delta, Egypt. El-Minia Sci Bull 11: 17-45.

24. Wang HF, Anderson MP (1995) Introduction to groundwater modeling: finite difference and finite element methods. Academic Press.

25. Aquaveo (2017) Groundwater Modeling System, GMS 10.2.3 (64-bit) Aquaveo, Provo.

26. Hesch W (2013) Understanding MODFLOW-USG: A Comparison between Structured MODFLOW and UnStructured MODFLOW [WWW Document], Schlumberger Water Serv.

27. Hefny K, Sahta A (2004) Underground water in Egypt, Ministry of Water Supplies and Irrigation, Egypt, in Annual Meeting, Egypt, Commission on Mineral and Thermal Waters, Handouts, pp. 11-23.

28. Anderson MP, Woessner WW, Hunt RJ (2015) Applied groundwater modeling: simulation of flow and advective transport. Academic Press.

29. El Haddad IM (2002) Hydrogeological studies and their environmental impact on future management and sustainable development of the new communities and their surroundings, east of the Nile Delta. PhD Thesis, University of Mansoura, Mansoura, Egypt.

30. Freeze RA, Witherspoon PA (1967) Theoretical analysis of regional groundwater flow: 2. Effect of water-table configuration and subsurface permeability variation. Water Resources Research. Wiley Online Library 3: 623-634.

31. Ramadan A, Ibrahim MB (2012) Inverse modeling of groundwater flow of Delta Wadi El-Arish. Journal of Water Resource and Protection. Scientific Research Publishing.

32. Doherty J (1994) PEST: a unique computer program for model-independent parameter optimisation, Water Down Under 94: Groundwater/Surface Hydrology Common Interest Papers; Preprints of Papers. Institution of Engineers, Australia, p: 551.

33. Doherty J (2010) EST Model-Independent Parameter Estimation User Manual: Fifth Edition, Watermark Numerical Computing.

34. Doherty JE, Hunt RJ, Tonkin MJ (2010) Approaches to highly parameterized inversion: A guide to using PEST for model-parameter and predictive-uncertainty analysis.

35. Sun N (2016) Drilling more wells or doing pumping test: investigating the relative value of water head and conductivity measurements in reducing inverse groundwater modeling error. The Pennsylvania State University The Graduate School.

36. Zare M, Koch M (2014) 3D-groundwater flow modeling of the possible effects of the construction of an irrigation/drainage network on water-logging in the Miandarband plain, Iran. J Soil Environ Sci 2: 2345-4090.

37. LeVeque RJ (2002) Finite volume methods for hyperbolic problems. Cambridge University Press.